CAUCHY – Jurnal Matematika Murni dan Aplikasi
Volume 11 (1) (2026), Pages 447-460
p-ISSN: 2086-0382; e-ISSN: 2477-3344

Stage-Structured Predator Model with Prey Protection: Application to Rice Plants–Leptocorisa oratorius

Safira Rahmah and Dian Savitri*

Department of Mathematics, Faculty of Mathematics and Natural Sciences, State University of Surabaya, Surabaya, Indonesia

Abstract

This study investigates a stage-structured predator–prey model consisting of prey, juvenile predators, and adult predators. The prey population follows logistic growth, while predation is described using a Holling type I functional response. Prey protection is incorporated through a protection parameter $(1 - m)$, representing the proportion of prey that successfully avoid predation by reducing the predation rate of adult predators. The model is analyzed by determining equilibrium points and examining their existence and stability. The results show four equilibrium points: total population extinction, prey-only equilibrium, juvenile predator extinction, and coexistence equilibrium. Predator extinction occurs when predation efficiency and predator reproduction are insufficient to compensate for predator mortality, whereas co-existence occurs when predation and conversion rates exceed mortality thresholds. Numerical simulations support the analytical results and demonstrate that increasing prey protection reduces predation pressure and may lead to predator decline, while appropriate predation efficiency promotes stable coexistence. These findings highlight the ecological importance of prey defense mechanisms in predator–prey interactions, particularly in rice–Leptocorisa oratorius.

Keywords: Age-structure; Equilibrium Point; Logistic Growth Model; Predator-prey Model; Protection of Prey; Stability Analysis.

1. Introduction

Rice plants (Oryza sativa L.) are one of the main staple food crops in Indonesia, and their productivity is strongly influenced by pest attacks. One of the major pests affecting rice production is the rice stink bug (Leptocorisa oratorius), which damages rice plants during the grain filling phase and can significantly reduce crop yield, potentially causing yield losses of up to 40 percent or more under severe infestation [1]. The life cycle of this pest consists of juvenile and adult stages, where adult stink bugs are generally more active in attacking rice plants. Variations in the population size of each stage strongly influence the level of crop damage, making stage-structured population analysis essential for effective pest management [2].

Mathematical modeling provides an effective approach to describe interactions between rice plants and pest populations. In this study, rice plants are considered as prey, while the rice stink bug population acts as the predator with juvenile and adult stages. The prey

***Corresponding author**. E-mail: diansavitri@unesa.ac.id

Submitted: January 26, 2026 Reviewed: February 06, 2026 Accepted: February 27, 2026
DOI: https://doi.org/10.18860/cauchy.v11i1.40733

population is assumed to follow logistic growth to represent environmental carrying capacity and intraspecific competition among rice plants [3, 4]. Several studies have developed predator–prey models incorporating stage structure and other ecological factors, including harvesting effects and environmental influences [5–8]. The predation process is modeled using a Holling type I functional response, which assumes that the predation rate increases linearly with prey density. This assumption is considered appropriate for rice stink bug interactions because the feeding activity of Leptocorisa oratorius mainly depends on the availability of rice grains and is not strongly limited by handling time.

In agricultural practice, farmers often apply simultaneous planting methods to reduce stink bug attacks. This practice creates a protective effect on rice plants by reducing pest accessibility to suitable plant stages [9]. In this study, prey protection is incorporated through a protection parameter that reduces the predation rate of adult predators. Several studies have shown that prey protection and refuge mechanisms can significantly influence the stability and persistence of predator–prey systems [10–13]. In addition, predator–prey models that consider prey protection and ecological interactions have also been investigated in various contexts [14–16].

Based on these considerations, this study aims to analyze the stability of a stage-structured predator–prey model involving rice plants and rice stink bugs. The model incorporates logistic prey growth, Holling type I predation, prey protection mechanisms, and predator age structure. The variables x,y, and z represent rice plant population, juvenile stink bug population, and adult stink bug population, respectively. The analysis includes determining equilibrium points, investigating their stability, and performing numerical simulations to examine the effects of protection and predation parameters on population dynamics.

2. Methods

In this study, a mathematical modeling approach was used to describe the interaction between prey and predator. This model was developed based on natural phenomena and supported by references from several previous studies. Specifically, this model describes the interaction between rice plants as prey and predators with a stage structure, including prey protection factors. The prey population is assumed to follow logistic growth, while predator-prey interactions are represented using Holling type I functional response. To formulate the model, a literature review of relevant previous studies was conducted.

At this stage, researchers consider the activity of *Leptocorisa oratorius* to be an active pest that damages rice plants. Based on a literature study referring to [2] and [9], it was found that *Leptocorisa oratorius* significantly disrupts rice growth and reduces crop productivity. Therefore, protective measures are needed to ensure optimal rice growth and a successful harvest for farmers.

In addition, the proposed model was developed by modifying the predator-prey model from previous studies, particularly those presented in [14, 16]. Several modifications were introduced to better reflect the biological characteristics of rice-pest interactions. These modifications include the application of logistic growth to prey populations to account for environmental constraints, the use of Holling type I functional responses to represent predation interactions, and the addition of stage structure to predator populations by dividing predators into juvenile and adult stages. In addition, a prey protection factor was incorporated into the model to represent the prey's ability to avoid predation. This protection mechanism was assumed to affect only adult predators, while juvenile predators were not affected by the protection effect.

After the model structure is established, the equilibrium points of the modified system are determined to identify conditions under which population density remains constant over time. The stability of each equilibrium point is then analyzed by linearizing the system using the Jacobian matrix and evaluating the eigenvalues obtained from the Jacobian matrix at each equilibrium point. These eigenvalues are used to determine whether the equilibrium points are stable or unstable. To complement the analytical results, numerical simulations are performed to describe population dynamics and observe the effects of parameter variations on system behavior. Finally, the results of analytical and numerical analyses are interpreted to provide a comprehensive understanding of the dynamics of interactions between prey and predator populations.

3. Results and Discussion

This section presents the main findings of the study by combining analytical results and numerical evidence. We first formulate the stage-structured predator–prey model with prey protection to clarify the biological assumptions and the role of each parameter. Next, we determine the equilibrium points and discuss their feasibility and local stability properties. Finally, numerical simulations are provided to illustrate the long-term dynamics and to support the theoretical stability analysis.

3.1. Mathematical Model

In this study, predator–prey interactions are represented by three populations consisting of prey $x(t)$, juvenile predators $y(t)$, and adult predators $z(t)$. The prey population represents rice plants, while predators represent stink bugs (Leptocorisa oratorius), which are divided into juvenile and adult stages according to their biological development. The prey population is assumed to grow logistically due to environmental limitations such as nutrients, space, and competition among rice plants.Predator–prey interactions follow a Holling type I functional response, which assumes that the predation rate increases linearly with prey density and leads to bilinear interaction terms between prey and predators in the model equations.

Juvenile predators are produced through successful predation events between juvenile predators and prey. Juvenile predators experience natural mortality and mature into adult predators. Adult predators increase through maturation of juvenile predators and reproduction resulting from successful predation by adult predators. Adult predators also experience natural mortality. Prey protection is incorporated through parameter m, representing the proportion of prey that successfully avoid predation by adult predators. The protection mechanism reduces the effective predation rate of adult predators by factor $(1-m)$. Based on the biological assumptions described above,the variables and parameters used in the model are presented in Table 1.

Table 1: Variables and parameters of the predator–prey model

Symbol	Description
$\frac{dx}{dt}$	Rate of change of prey population at time t.
$\frac{dy}{dt}$	Rate of change of juvenile predators at time t
$\frac{dz}{dt}$	Rate of change of adult predators at time t
r	the maximum growth rate of prey.
k	carrying capacity.
λ_1	Predation rate of juvenile predators on prey.
β_1	Predation rate of adult predators on prey.
m	Prey protection factor.
λ_2	Conversion rate of consumed prey into juvenile predators.
η	Maturation rate from juvenile to adult predators.
δ_1	Natural mortality rate of juvenile predators.
β_2	Conversion rate of consumed prey into adult predators.

Based on the biological mechanisms, the system is formulated as follows:

$$\frac{dx}{dt} = rx\left(1 - \frac{x}{k}\right) - \lambda_1 xy - \beta_1(1-m)xz \tag{1}$$

$$\frac{dy}{dt} = \lambda_2 xy - \eta y - \delta_1 y \tag{2}$$

$$\frac{dz}{dt} = \eta y + \beta_2(1-m)xz - \delta_2 z \tag{3}$$

Eq. (1) represents the rate of change in the prey population. The first term describes logistic growth with intrinsic growth rate r and carrying capacity k. The second and third terms represent the decline in the prey population due to predation by juvenile and adult predators, respectively. The factor $(1-m)$ reflects the prey's defense mechanism, which reduces the effectiveness of predation by adult predators.

Eq. (2) describes the rate of change in the juvenile predator population. The population increases through successful predation on prey at a conversion rate λ_2. The population decreases due to maturation into adult predators at a rate η and natural death at a rate δ_1.

Eq. (3) represents the rate of change in the adult predator population. The adult predator population increases due to the maturation of young predators and reproduction resulting from successful predation at the conversion rate β_2. The population decreases due to natural mortality at the rate δ_2.

Where x, y and z are respectively the densities of prey and two predator population at time t and x(0), y(0), z(0)> 0. To simplify the equations of the three mathematical models, the equations are converted into factors so that they become:

$$\frac{dx}{dt} = x\left(r\left(1-\frac{x}{k}\right) - \lambda_1 y - \beta_1(1-m)z\right) \tag{4}$$

$$\frac{dy}{dt} = y(\lambda_2 x - \eta - \delta_1) \tag{5}$$

$$\frac{dz}{dt} = z(\beta_2(1-m)x - \delta_2) + \eta y \tag{6}$$

3.2. Existence and Stability Analysis of Equilibrium Points

In this section, the equilibrium point of model in (4)-(6) is obtained by solving [17]:

$$\frac{dx}{dt} = \frac{dy}{dt} = \frac{dz}{dt} = 0$$

Thus, from system Eqs. (4)-(6), the following equilibrium points are obtained:

1. A trivial equilibrium point $E_0 : (0, 0, 0)$ always exists. This point describes the extinction of all populations.
2. A non-predator equilibrium point
$$E_1 : (k, 0, 0)$$
always exists. This equilibrium represents a predator-free condition where the prey population reaches the environmental carrying capacity.
3. An equilibrium point when juvenile predators are absent
$$E_2 : \left(\frac{\delta_2}{\beta_2(1-m)}, 0, \frac{r(\beta_2(1-m)k - \delta_2)}{\beta_1(1-m)\beta_2(1-m)k}\right)$$
This equilibrium describes predator–prey interaction involving only adult predators. The equilibrium E_2 exists biologically if
$$m < 1 \text{ and } \beta_2(1-m)k > \delta_2$$
These conditions indicate that adult predators can survive when the effective predation rate exceeds their natural mortality.
4. A coexistence equilibrium point $E_3 : (x^*, y^*, z^*)$ where all populations survive simultaneously. To simplify notation, define
$$D = \eta\beta_1(1-m)\lambda_2 - \beta_2(1-m)(\eta+\delta_1)\lambda_1 + \lambda_2\delta_2\lambda_1.$$

The coexistence equilibrium is given by

$$x^* = \frac{\eta + \delta_1}{\lambda_2},$$
$$y^* = \frac{r(-k\lambda_2 + \eta + \delta_1)\,[\beta_2(1-m)(\eta+\delta_1) - \lambda_2\delta_2]}{D\,k\,\lambda_2},$$
$$z^* = -\frac{\eta r(-k\lambda_2 + \eta + \delta_1)}{D\,k}.$$

The equilibrium E_3 is biologically feasible if

$$k\lambda_2 > \eta + \delta_1,\ D > 0, \text{ and } \beta_2(1-m)(\eta+\delta_1) > \lambda_2\delta_2$$

These feasibility conditions indicate that coexistence occurs when prey growth is sufficient to support predator maturation and reproduction, while predator mortality remains lower than the effective predation and conversion rates. Under these conditions, prey, juvenile predators, and adult predators can coexist in long-term population dynamics.

Now, the local stability dynamics of system (4)-(6) around each equilibrium point are analyzed. The Jacobian matrix for system (4)-(6) is defined as follows [18]:

$$J_{(x,y,z)} := \begin{bmatrix} r\left(1-\frac{2x}{k}\right) - \lambda_1 y - \beta_1(1-m)z & -\lambda_1 x & -\beta_1(1-m)x \\ \lambda_2 y & \lambda_2 x - \eta - \delta_1 & 0 \\ \beta_2(1-m)z & \eta & \beta_2(1-m)x - \delta_2 \end{bmatrix} \tag{7}$$

By evaluating the Jacobian matrix at each equilibrium point, the local stability properties of E_0, E_1, E_2, and E_3 are obtained as follows.

Theorem 1. *The equilibrium point E_0 is always unstable (saddle point).*

Proof. Evaluating the Jacobian matrix at $E_0 = (0,0,0)$ yields

$$J_{(E_0)} := \begin{bmatrix} r & 0 & 0 \\ 0 & -(\eta+\delta_1) & 0 \\ 0 & \eta & -\delta_2 \end{bmatrix}.$$

The characteristic equation of $J_{(E_0)}$ is obtained from

$$\det(J_{(E_0)} - \mu I) = 0,$$

which gives

$$(\mu - r)(\mu + \eta + \delta_1)(\mu + \delta_2) = 0.$$

Thus, the eigenvalues are

$$\mu_1 = r, \quad \mu_2 = -(\eta+\delta_1), \quad \mu_3 = -\delta_2.$$

Since $r > 0$, one eigenvalue is positive, while the other two eigenvalues are always negative. Therefore, the equilibrium point E_0 has eigenvalues with opposite signs, implying that E_0 is a saddle point and hence locally unstable. □

Theorem 2. *The equilibrium point $E_1 = (k,0,0)$ is locally asymptotically stable if $k\lambda_2 < \eta + \delta_1$ and $\beta_2(1-m)k < \delta_2$.*

Proof. Evaluating the Jacobian matrix (7) at equilibrium point E_1 gives

$$J_{(E_1)} := \begin{bmatrix} -r & -\lambda_1 k & -\beta_1(1-m)k \\ 0 & k\lambda_2 - \eta - \delta_1 & 0 \\ 0 & \eta & \beta_2(1-m)k - \delta_2 \end{bmatrix}.$$

Since $J_{(E_1)}$ is triangular, the characteristic equation is obtained from the diagonal entries:

$$(\mu + r)(\mu - (k\lambda_2 - \eta - \delta_1))(\mu - (\beta_2(1-m)k - \delta_2)) = 0.$$

Hence, the eigenvalues are

$$\mu_1 = -r,$$
$$\mu_2 = k\lambda_2 - \eta - \delta_1,$$
$$\mu_3 = \beta_2(1-m)k - \delta_2.$$

Since $r > 0$, we have $\mu_1 < 0$. The remaining eigenvalues are negative if

$$k\lambda_2 < \eta + \delta_1 \quad \text{and} \quad \beta_2(1-m)k < \delta_2.$$

Therefore, all eigenvalues of $J(E_1)$ have negative real parts and E_1 is locally asymptotically stable. □

Theorem 3. *Under the feasibility condition*

$$m < 1 \quad \textit{and} \quad \beta_2(1-m)k > \delta_2,$$

two eigenvalues of $J(E_2)$ are negative. Moreover, the equilibrium point

$$E_2 = \left(\frac{\delta_2}{\beta_2(1-m)}, 0, \frac{r(\beta_2(1-m)k - \delta_2)}{\beta_1(1-m)\beta_2(1-m)k} \right)$$

is unstable (saddle) if and only if

$$\frac{\delta_2\lambda_2}{\beta_2(1-m)} > \eta + \delta_1.$$

Proof. The Jacobian matrix (7) evaluated at E_2 is given by

$$J(E_2) := \begin{bmatrix} J_{11} & J_{12} & J_{13} \\ 0 & J_{22} & 0 \\ J_{31} & \eta & 0 \end{bmatrix}.$$

Because the matrix has a triangular block structure, one eigenvalue is directly obtained as

$$\mu_1 = J_{22} = \frac{\delta_2\lambda_2}{\beta_2(1-m)} - \eta - \delta_1.$$

The remaining eigenvalues are obtained from the quadratic equation

$$\mu^2 - J_{11}\mu - \eta J_{13} = 0.$$

From the expression of E_2, we have

$$x_2 = \frac{\delta_2}{\beta_2(1-m)}.$$

Under the feasibility condition $\beta_2(1-m)k > \delta_2$, it follows that $x_2 < k$.
Substituting x_2 into J_{11} yields

$$J_{11} = r\left(1 - \frac{2\delta_2}{\beta_2(1-m)k}\right) - \frac{r(\beta_2(1-m)k - \delta_2)}{\beta_2(1-m)k} = -\frac{r\delta_2}{\beta_2(1-m)k} < 0.$$

Moreover,

$$J_{13} = -\frac{\beta_1(1-m)\delta_2}{\beta_2(1-m)} < 0,$$

since all parameters are positive. Hence,

$$-\eta J_{13} > 0.$$

For the quadratic equation

$$\mu^2 - J_{11}\mu - \eta J_{13} = 0,$$

the sum and product of its roots satisfy

$$\mu_2 + \mu_3 = J_{11} < 0, \qquad \mu_2\mu_3 = -\eta J_{13} > 0.$$

Since the product of the roots is positive and their sum is negative, it follows that

$$\mu_2 < 0 \quad \text{and} \quad \mu_3 < 0.$$

Thus, two eigenvalues of $J(E_2)$ are strictly negative under the feasibility condition.
Consequently, the stability of E_2 is determined solely by the sign of

$$\mu_1 = \frac{\delta_2\lambda_2}{\beta_2(1-m)} - \eta - \delta_1.$$

If

$$\frac{\delta_2\lambda_2}{\beta_2(1-m)} > \eta + \delta_1,$$

then $\mu_1 > 0$. Hence, $J(E_2)$ possesses exactly one positive eigenvalue and two negative eigenvalues, implying that E_2 is a saddle equilibrium and therefore unstable.
Otherwise, if

$$\frac{\delta_2\lambda_2}{\beta_2(1-m)} < \eta + \delta_1,$$

then $\mu_1 < 0$ and all three eigenvalues are negative. In this case, E_2 is locally asymptotically stable. □

Theorem 4. *The coexistence equilibrium point $E_3 = (x^*, y^*, z^*)$ is locally asymptotically stable if the Routh–Hurwitz conditions are satisfied.*

Proof. The Jacobian matrix (7) evaluated at the coexistence equilibrium point E_3 is given by

$$J_{(E_3)} = \begin{bmatrix} V_{11} & V_{12} & V_{13} \\ V_{21} & V_{22} & 0 \\ V_{31} & \eta & V_{33} \end{bmatrix}$$

where

$$\begin{aligned}
V_{11} &= r\left(1 - \frac{2x^*}{k}\right) - \lambda_1 y^* - \beta_1(1-m)z^*, \\
V_{12} &= -\lambda_1 x^*, \\
V_{13} &= -\beta_1(1-m)x^*, \\
V_{21} &= \lambda_2 y^*, \\
V_{22} &= \lambda_2 x^* - \eta - \delta_1, \\
V_{31} &= \beta_2(1-m)z^*, \\
V_{33} &= \beta_2(1-m)x^* - \delta_2.
\end{aligned}$$

The characteristic equation of $J_{(E_3)}$ is obtained from

$$\det(\mu I - J_{(E_3)}) = 0,$$

which yields the cubic polynomial

$$\mu^3 + A_1\mu^2 + A_2\mu + A_3 = 0$$

with coefficients

$$\begin{aligned}
A_1 &= -(V_{11} + V_{22} + V_{33}), \\
A_2 &= V_{11}V_{22} + V_{11}V_{33} + V_{22}V_{33} - V_{12}V_{21} - V_{13}V_{31}, \\
A_3 &= -\det(J_{(E_3)}).
\end{aligned}$$

According to the Routh–Hurwitz stability criterion for nonlinear dynamical systems [19], the equilibrium point E_3 is locally asymptotically stable if the following conditions hold

$$A_1 > 0, \quad A_2 > 0, \quad A_3 > 0, \quad A_1A_2 > A_3.$$

These conditions ensure that all eigenvalues of the characteristic equation have negative real parts. Therefore, if the above Routh–Hurwitz conditions are satisfied, the equilibrium point E_3 is locally asymptotically stable. □

Due to the complexity of the analytical expressions, numerical simulations are performed to verify the stability conditions.

3.3. Numerical Simulations

In this Section, Numerical simulations were conducted in Python using Google Colab. The system was solved numerically with the `solve_ivp` function in SciPy using the Runge–Kutta (RK45) method, and the results were visualized with Matplotlib. The simulations were performed over the time interval $t \in [0, 400]$ with 6000 evaluation points, using the default relative tolerance of 10^{-3} and absolute tolerance of 10^{-6}. Numerical simulations were conducted to support the analysis and display changes in the equilibrium point solution. The parameter values used must first meet certain conditions for the existence of an equilibrium point. In this case, all parameter values were obtained from several previous journal references. The parameter values are shown in the following table:

For the simulation, we used the parameters from Table 2. The following numerical simulation example is divided into two parts. The first part is the numerical continuity of the parameter values. The second part explains the model solution in the form of a time series graph and phase portrait.

Table 2: Parameter Values Used in Numerical Simulations

Parameter	Description	Value	References
r	the maximum growth rate of prey	0.5	[16]
k	Carrying Capacity	20	[20]
λ_1	Predation rate of juvenile predators on prey	0.2	[20]
λ_2	Conversion rate of consumed prey into juvenile predators	0.5	[20]
β_1	Predation rate of adult predators on prey	0.2	[16]
β_2	Conversion rate of consumed prey into adult predators	0.1	[16]
m	Prey protection factor	0.0051	[14]
η	Maturation rate from juvenile to adult predators	0.06	[21]
δ_1	Natural mortality rate of juvenile predators	0.51	[16]
δ_2	Natural mortality rate of adult predators	0.5	[16]

In this section, For the numerical simulation, we take same parameter values in Table 2. Using these parameter values, it can be shown that the equilibirum point E_1, E_2, and E_3 of the system in Eqs. (1)–(2) Exist. All equilibrium points are $E_1 = (20{,}0{,}0)$ unstable with eigenvalue $\lambda_1 = -0.5$, $\lambda_2 = 1.5$, $\lambda_3 = 9.43$, $E_2 = (5{,}0{,}1.875000000)$ unstable with eigenvalue, $\lambda_1 = -0.0625000000000000 + 0.428478412525065I$, $\lambda_2 = -0.0625000000000000 - 0.42847841252506I$, $\lambda_3 = 1.93000000000000$, $E_3 = (1.140000000{,}2.040347534{,}0.3171524664)$ stable with eigenvalue $\lambda_1 = -0.000272753532443853 + 0.500605439089338I$, $\lambda_2 = -0.000272753532443853 - 0.500605439089338I$, $\lambda_3 = -0.413954493015112$

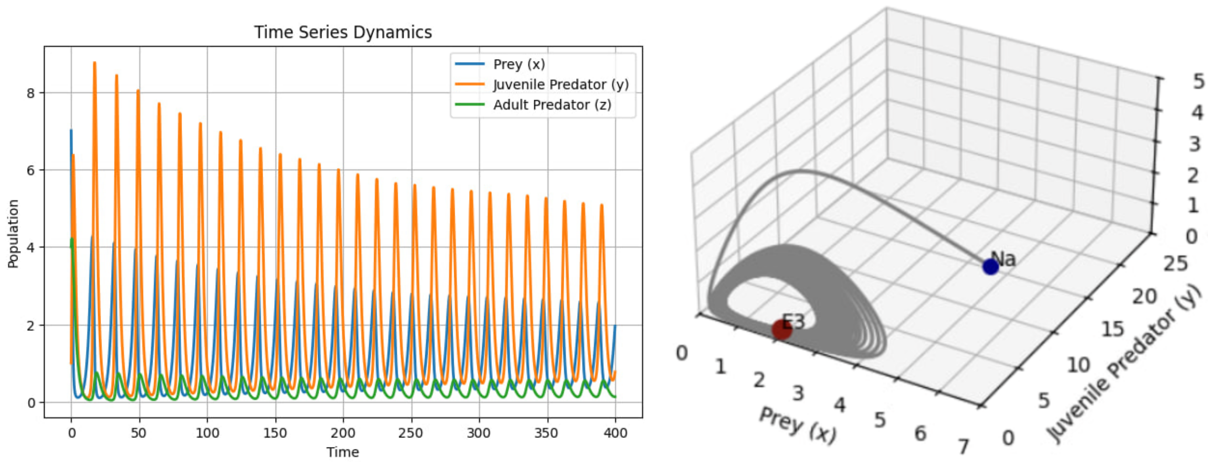

(a) Time Series Graph of Prey and Predators **(b)** The phase Potraits for Parameter in Table 1

Fig. 1: The dynamics of the solution system tend to E_3 stable. Phase portraits were plotted using identical axis limits (x : 0–7, y : 0–25, z : 0–5) and a consistent viewpoint (elevation 30°, azimuth −60°).

Based on the results of numerical simulations in Fig. 1a, it can be seen that the prey population $x(t)$, young predator population $y(t)$, and adult predator population $z(t)$ exhibit oscillatory patterns with decreasing amplitudes that eventually approach constant values. This pattern indicates that the system is approaching a stable coexistence equilibrium point. this dynamic shows that the interior equilibrium point E_3 is asymptotically stable. This is demonstrated by the behavior of the system solution, which, for a sufficiently long time, approaches the equilibrium value after experiencing population fluctuations in the initial phase.

Biologically, this phenomenon describes the dynamic interaction between rice plants as a food source and leptocorisa oratorius as pests. Population fluctuations occur due to changes in food availability and predation pressure. In the long term, the system shows stable coexistence between rice and leptocorisa oratorius, indicating that ecosystems can achieve natural equilibrium without causing the extinction of either population.

As shown in Fig. 1b, the boundary equilibria $E_1 = (20, 0, 0)$ and $E_2 = (5, 0, 1.875000000)$ remain unstable. In contrast, the interior equilibrium $E_3 = (1.140000000, 2.040347534, 0.3171524664)$ is stable, with eigenvalues $\lambda_{1,2} = -0.000272753532443853 \pm 0.500605439089338\,i$, $\lambda_3 = -0.413954493015112$. The phase portrait indicates that the trajectories of the system converge to the stable equilibrium E_3. Next, we choose different parameter control values, namely $\beta_1 = 0.05$ and $\lambda_1 = 0.1$.

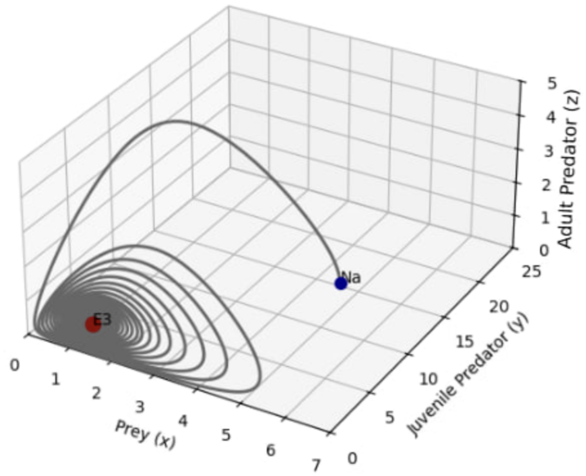

Fig. 2: Phase portrait 3D for parameter $\beta_1 = 0.05$. Phase portraits were plotted using identical axis limits (x : 0–7, y : 0–25, z : 0–5) and a consistent viewpoint (elevation 30°, azimuth −60°).

In Fig. 2, with initial condition Na = $[x(0) = 1.14,\ y(0) = 2, z(0) = 0.3]$ for $\beta_1 = 0.05$ we find the interior equlibirum E_1=(20,0,0) and E_2=(5,0,7.500000000) unstable. The interior equlibirum E_3 = (1.140000000,2.269314214,0.3527431421) its stabil with eigenvalues λ_1 =-0.0104123857834755 + 0.513231762255673I, λ_2=-0.0104123857834755 - 0.513231762255673, and λ_3=-0.393675228333049. The phase portrait shows that at β_1=0.05, the system has an asymptotically stable coexistence equilibrium point E_3, while points E_1 and E_2 are unstable. Biologically, this condition indicates that rice and brown planthopper populations can coexist stably when the level of adult predator attacks on rice is relatively low.

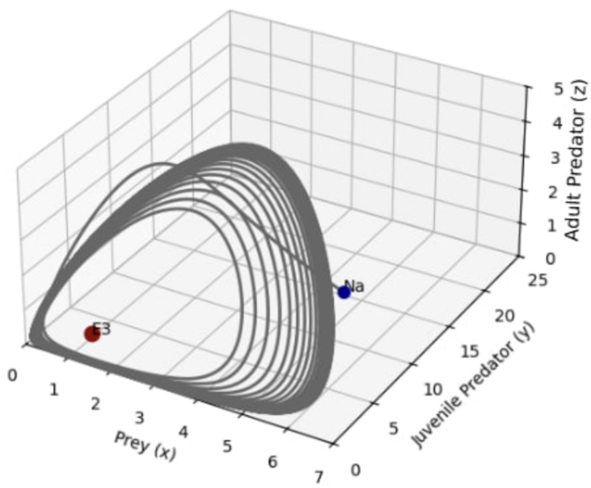

Fig. 3: Phase portrait 3D for parameter $\lambda_1 = 0.1, \beta_1 = 0.2$. Phase portraits were plotted using identical axis limits (x : 0–7, y : 0–25, z : 0–5) and a consistent viewpoint (elevation 30°, azimuth −60°).

In Fig. 3, a phase portrait of the system with parameter value λ_1=0.1 is presented. we get the equilibirum E_1 (20,0,0), E_2 (5,0,1.875000000) and E_3 (1.140000000, 3.596818182, 0.5590909091) Unstable. Under these conditions, the system exhibits significant instability. This is evident from the phase portrait, where the trajectories do not converge to any equilibrium point but instead display large-amplitude oscillatory behavior away from the interior equilibrium. The low value of λ_1 reduces the damping effect in the system, causing population fluctuations to persist over time. Biologically, this implies that the prey and age-structured predator populations experience recurrent population cycles with large amplitudes, preventing the system from reaching a stable equilibrium state.

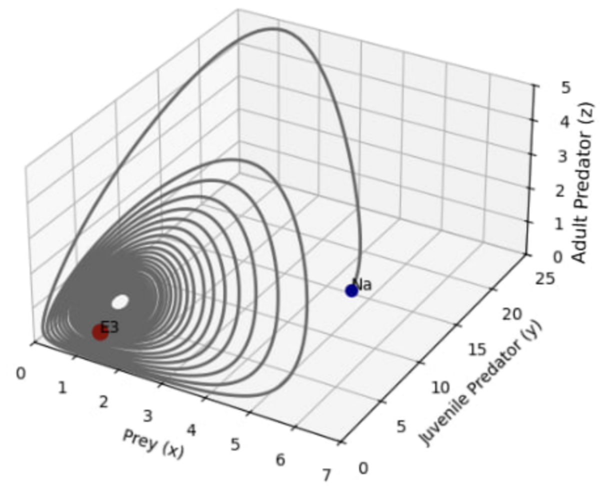

Fig. 4: Phase portrait 3D for parameter $\lambda_1 = 0.1, \beta_1 = 0.05$. Phase portraits were plotted using identical axis limits (x : 0–7, y : 0–25, z : 0–5) and a consistent viewpoint (elevation 30°, azimuth −60°).

In Fig. 4, with a value of $\beta_1 = 0.05$ and λ_1=0.1, we get the equilibirum E_1 (20,0,0), E_2 (5,0,7.500000000) unstable remains itself. The Interior equilibrium E_3(1.140000000, 4.374975962, 0.6800480769) stable with eigenvalue λ_1 = -0.00681564374367188 + 0.508665011793265I, λ_2=-0.00681564374367188 - 0.508665011793265I, λ_3=-0.400868712552656. When the parameters $\lambda_1 = 0.1$ and $\beta_1 = 0.05$, the phase portrait shows that the solution trajectory gradually converges toward the interior equilibrium point E_3. This indicates that E_3 is an asymptotically stable equilibrium point. the decrease in the value of β_1 weakens the intensity of nonlinear interactions in the system, so that previously undamped population oscillations become damped and converge to a steady state. This condition shows that the β_1 parameter plays an important role in determining the stability of the system and can control the occurrence of population oscillations.

Biologically, a smaller β_1 value reflects a decrease in the level of adult stink bug attacks on rice plants, thereby reducing pressure on the prey and allowing the population dynamics of rice, young stink bugs, and adult stink bugs to reach a stable equilibrium. Thus, β_1 is a key parameter in maintaining the stability of population coexistence in the system.

4. Conclusion

This study discusses a predator–prey model with life stage structures in predators and prey protection mechanisms. In this model, the prey population follows logistic growth, while predators are differentiated into juvenile and adult stages. Mathematical analysis shows the existence of four equilibrium points, namely the total extinction point E_0, the prey-only equilibrium point E_1, the equilibrium point without juvenile predators E_2, and the coexistence point E_3. Stability analysis results show that E_0 is always unstable, E_2 is generally unstable, while the stability of E_1 and E_3 is highly dependent on the value of the interaction parameters in the system.

Numerical simulations confirm that the long-term dynamics of the system are mainly determined by the stability of the coexistence point E_3. For certain parameter values, the system exhibits large undamped population oscillations, while under other parameter conditions, the solution trajectory asymptotically converges to E_3. In particular, a decrease in the adult predator predation rate parameter β_1 was found to dampen population oscillations and stabilize the system, allowing all populations to remain in equilibrium. This confirms the important role of β_1 as a parameter controlling the stability of the system.

Although the prey protection mechanism is modeled through the parameter $(1 - m)$, this study has not conducted a systematic parametric or bifurcation analysis of the parameter m. Therefore, conclusions regarding the direct effect of prey protection levels on predator extinction are limited to model indications and are not claimed to be definitive results. Further analysis is needed to determine the threshold of the parameter m that can trigger changes in stability or predator extinction.

From an application perspective, the results of the coexistence point stability analysis provide theoretical insights into agricultural pest management strategies, particularly simultaneous planting practices. In this context, simultaneous planting can be viewed as a mechanism that influences interaction parameters in the system, thereby helping to keep population dynamics in a stable regime and preventing excessive pest population oscillations. Thus, this model provides a mathematical framework that can support the formulation of ecosystem stability-based pest control strategies, while also opening up opportunities for further research through bifurcation and parameter sensitivity analysis.

CRediT Authorship Contribution Statement

Safira Rahmah: Conceptualization, Methodology, Formal Analysis, Numerical Simulations, Data Curation, Writing - Original Draft, Visualization. **Dian Savitri**: Conceptualization, Methodology, Validation, Writing - Review and Editing, Project Administration.

Declaration of Generative AI and AI-assisted technologies

No generative AI or AI-assisted technologies were used during the preparation of this manuscript.

Declaration of Competing Interest

The authors declare no competing interests.

Funding and Acknowledgments

This research did not receive any specific grant from funding agencies in the public, commercial, or not-for-profit sectors.

Data and Code Availability

The data and code supporting the findings of this study are available from the corresponding author upon reasonable request and subject to confidentiality agreements.

References

[1] Nasrah K. Bajber, Moh. Hibban Toana, and Asrul Asrul. "Populasi Walang Sangit Leptocorisa acuta Thunberg (Hemiptera: Alydidae) serta Produksi Dua Varietas Tanaman Padi di Kecamatan Toribulu". In: *AGROTEKBIS: Jurnal Ilmu Pertanian* 8.6 (2020), pp. 1274–1282. http://jurnal.faperta.untad.ac.id/index.php/agrotekbis/article/view/886.

[2] Dinas Pertanian Kabupaten Buleleng. *Strategi Pengendalian OPT Walang Sangit (Leptocorisa spp.) pada Tanaman Padi*. 2023. https://www.distan.bulelengkab.go.id/strategi-pengendalian-opt-walang-sangit.

[3] S. Sunarsih and F. N. Hidayati. “Model Pertumbuhan Logistik Predator dan Prey pada Populasi Prey dan Solusi Kesetimbangan”. In: *Jurnal Sains dan Matematika* 18.1 (2010), pp. 7–12. https://ejournal.undip.ac.id/index.php/sm/article/view/3118.

[4] Suqi Ma and Meisheng Li. “Hopf Bifurcation for a Predator–Prey System with θ Logistic Growth”. In: *International Journal of Modern Nonlinear Theory and Application* 14.4 (2025), pp. 96–109. DOI: 10.4236/ijmnta.2025.144006.

[5] Luis Suarez, Maria K. Cameron, William F. Fagan, and Doron Levy. *A Predator–Prey Model with Age-Structured Role Reversal*. arXiv:2502.19748. 2025. https://arxiv.org/abs/2502.19748.

[6] Marcel Mohr, Maria V. Barbarossa, and Christina Kuttler. *Predator–Prey Interactions, Age Structures and Delay Equations*. arXiv:1308.2532. 2013. https://arxiv.org/abs/1308.2532.

[7] Rima A. Pratiwi, Agus Suryanto, and Trisilowati. “Numerical Simulation of Leslie–Gower Predator–Prey Model with Stage-Structure on Predator”. In: *Journal of Experimental Life Science* 8.3 (2018), pp. 202–206. DOI: 10.21776/ub.jels.2018.008.03.011.

[8] Hasan S. Panigoro, R. Resmawan, Amelia T. R. Sidik, Nurdia Walangadi, Apon Ismail, and Cabelita Husuna. “A Fractional-Order Predator–Prey Model with Age Structure on Predator and Nonlinear Harvesting on Prey”. In: *Jambura Journal of Mathematics* 4.2 (2022), pp. 355–366. DOI: 10.34312/jjom.v4i2.15220.

[9] Dinas Pertanian Kabupaten Tulang Bawang. *Pengendalian Hama Walang Sangit pada Tanaman Padi*. Accessed: 2025-09-12. 2021. https://distani.tulangbawangkab.go.id/pengendalian-hama-walang-sangit-pada-tanaman-padi.

[10] Arild Wikan and Orjan Kristensen. “An Analysis of Discrete Stage-Structured Prey and Predator Population Models”. In: *Discrete Dynamics in Nature and Society*, 9475854 (2017). DOI: 10.1155/2017/9475854. https://onlinelibrary.wiley.com/doi/10.1155/2017/9475854.

[11] Ahmed B. Ashine and Dawit M. Gebru. “Mathematical Modeling of a Predator–Prey Model with Modified Leslie–Gower and Holling-Type II Schemes”. In: *Global Journal of Science Frontier Research: Mathematics and Decision Sciences* 17.3 (2017), pp. 21–40. https://journalofscience.org/index.php/GJSFR/article/view/2023.

[12] Sinan Kapcak, Saber Elaydi, and Unal Ufuktepe. “Stability of a Predator–Prey Model with Refuge Effect”. In: *Journal of Difference Equations and Applications* 22.7 (2016), pp. 989–1004. DOI: 10.1080/10236198.2016.1170823.

[13] Sahabuddin Sarwardi, Prashanta K. Mandal, and Santanu Ray. “Dynamical Behaviour of a Two-Predator Model with Prey Refuge”. In: *Journal of Biological Physics* 39.4 (2013), pp. 701–722. DOI: 10.1007/s10867-013-9327-7.

[14] Zhaozhi Ma, Fengde Chen, and Chengqing Wu. “Dynamic Behaviors of a Lotka–Volterra Predator–Prey Model Incorporating a Prey Refuge”. In: *Applied Mathematics and Computation* 219.15 (2013), pp. 7945–7953. DOI: 10.1016/j.amc.2013.02.033.

[15] Laras K. M. Putri, Dian Savitri, and Abadi Abadi. “Dynamical Behavior in Prey–Predator Model with Mutualistic Protection for Prey”. In: *Jambura Journal of Biomathematics* 4.2 (2023), pp. 103–109. DOI: 10.37905/jjbm.v4i2.21541.

[16] Lazarus K. Beay and Maryone Saija. “A Stage-Structure Rosenzweig–MacArthur Model with Effect of Prey Refuge”. In: *Jambura Journal of Biomathematics* 1.1 (2020). DOI: 10.34312/jjbm.v1i1.6891.

[17] Lawrence Perko. *Differential Equations and Dynamical Systems*. Springer, 2001. DOI: 10.1007/978-1-4613-0003-8.

[18] Jack K. Hale and Huseyin Kocak. *Dynamics and Bifurcations*. Springer, 1991. DOI: 10.1007/978-1-4612-4426-4.

[19] R. K. Upadhyay and S. R. K. Iyengar. "Complex Dynamics of Eco-Epidemiological Models". In: *Nonlinear Analysis: Modelling and Control* 16.4 (2011), pp. 441–457.

[20] Nishant Juneja and Kulbhushan Agnihotri. "Dynamical Behavior of Prey–Predator System with Alternative Food for Predator". In: *International Journal on Emerging Technologies* 10.1 (2019), pp. 143–147. %5Curl%7Bhttps://www.researchtrend.net/ijet/pdf/Dynamical%20Behavior%20of%20Prey%20Predator%20System%20with%20Alternative%20Food%20for%20Predator%20NISHANT%20JUNEJA.pdf%7D.

[21] Ainun S. Al Idrus, Ayub P. Abd. Gani, and Nurlaila Zaid. "Analisis Dinamik Model Predator–Prey dengan Struktur Usia dan Perilaku Anti-Predator". In: *Research in the Mathematical and Natural Sciences* 1.2 (2022), pp. 22–29. DOI: 10.55657/rmns.v1i2.63.